

ACKNOWLEDGMENT

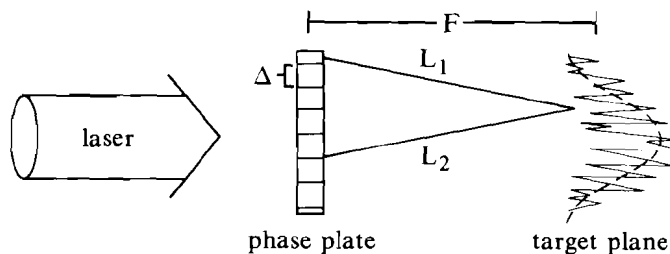
This work was supported by the U.S. Department of Energy Office of Inertial Fusion under agreement No. DE-FC03-85DP40200 and by the Laser Fusion Feasibility Project at the Laboratory for Laser Energetics, which has the following sponsors: Empire State Electric Energy Research Corporation, New York State Energy Research and Development Authority, Ontario Hydro, and the University of Rochester. Such support does not imply endorsement of the content by any of the above parties.

REFERENCES

1. LLE Review **31**, pp. 106ff and 114ff (1987); S. Skupsky and T. Kessler (accepted for publication in *Opt. Commun.*).
2. LLE Review **36**, pp. 158ff (1988); LLE Review **33**, pp. 1ff (1987).
3. W. Seka, S. D. Jacobs, J. E. Rizzo, R. Boni, and R. S. Craxton, *Opt. Commun.* **34**, 469 (1980); R. S. Craxton, *ibid.* **34**, 474 (1980).
4. J. B. Trenholme and K. R. Manes, Lawrence Livermore National Laboratory Report UCRL-51413 (1972).
5. R. S. Craxton, *IEEE J. Quantum Electron.* **J-QE-17**, 1771 (1981).

1.C Improved Laser-Beam Uniformity by the Angular Dispersion of Frequency-Modulated Light

A new technique is being examined to improve the quality of OMEGA laser beams beyond the level that has already been achieved with distributed phase plates (DPP's).¹ These phase plates break each beam into beamlets whose diffraction-limited size equals the size of the target.² However, superimposed on the smooth diffraction-limited intensity envelope is a rapidly varying intensity structure from the interference between the different beamlets (Fig. 37.20). Once a plasma atmosphere has been established around the target, much of the short-wavelength interference structure in the laser-energy deposition is expected to be smoothed by thermal conduction within the target as heat is transported from the place of energy deposition to the ablation surface. However, before thermal smoothing becomes effective, this structure could imprint itself on the target surface and "seed" the Rayleigh-Taylor instability, much like a target surface imperfection. The longer-wavelength interference structure will never be adequately smoothed and could drive a distorted implosion. The goal of the work described here is to develop a technique to reduce the magnitude of the interference structure, while retaining the smooth intensity envelope.



TC2429

Fig. 37.20

The phase-plate intensity pattern in the focal plane consists of a diffraction-limited envelope superimposed upon a rapidly varying structure caused by the interference between rays from different DPP elements.

The strategy employed is to shift the interference pattern on a time scale Δt that is short compared to the characteristic hydrodynamic response time of the target. At any instant of time, a highly modulated intensity pattern will be present, but the time-averaged intensity over Δt will be smooth. The interference pattern can be shifted (or changed) by rapidly shifting the beam, or rapidly changing the relative phases between the individual beamlets. An example of the latter approach is induced spatial incoherence (ISI).³ But ISI might not be a good candidate for a frequency-tripled glass-laser system such as OMEGA, since the required "chaotic" bandwidth could be difficult to triple efficiently and would produce high-intensity temporal spikes within the laser that could damage the laser glass. Therefore, we have been considering an alternate scheme, smoothing by spectral dispersion (SSD) of the laser light. Like ISI, it requires a bandwidth, but the smoothing mechanism is different, permitting the use of a nonchaotic bandwidth and allowing high-efficiency frequency tripling. A possible method of implementing SSD on a limited scale, with current technology, is described below. This relatively simple technique will not eliminate all the interference structure, but it takes a major step in that direction without degrading the performance of the high-power frequency-tripled laser system. Further improvements in uniformity are possible with other variations of SSD that are presently under investigation.

Implementation Considerations for SSD

The general concept of SSD is to spectrally disperse broad-bandwidth light onto a phase plate so that, ideally, each element of the DPP is irradiated by a different frequency.⁴ The relative phase between rays from different phase-plate elements will then vary in time according to their frequency differences. The larger the bandwidth, the more rapidly the structure will change and the more rapidly the time-averaged intensity will smooth. However, if some phase-plate elements have the same "color" (frequency), a residual interference structure will be produced that will not smooth.

To implement this scheme on a laser system such as OMEGA, a number of key requirements must be met: (1) generation of bandwidth that will not damage the laser glass; (2) dispersion of the bandwidth

across the DPP elements together with high-efficiency frequency tripling; (3) identification of a dispersing configuration that will not significantly distort the beam; and (4) obtaining the improved uniformity over a sufficiently small averaging time.

1. Bandwidth Source

One form of bandwidth that can be easily propagated through a glass laser system is generated by phase modulation of the beam. The phase-modulated electric field is of the form⁵ $E(t) = E_0(t)e^{i\Phi(t)}$, where the entire effect of bandwidth on the original field E_0 is contained in the time-varying phase. The laser intensity varies as $|E(t)|^2 = |E_0(t)|^2$ and contains no additional high-intensity spikes from the interference between different frequencies. This would not be true for the chaotic form of bandwidth required by ISI in which the different modes have random phases (i.e., $E(t) = \sum a_n e^{i\omega_n t + \phi_n}$ where ϕ_n is random). One relatively simple form of phase modulation can be obtained by passing the laser beam through an electro-optical (E-O) crystal with an imposed oscillating electric field. The effect is to produce a laser electric field of the form:

$$E(t) = E_0 e^{i\omega t + i\delta \sin \omega_m t}, \quad (1)$$

where δ and ω_m are the modulation amplitude and angular frequency of the E-O device, and ω is the fundamental angular frequency of the laser. By expanding the exponential term in a Bessel function series⁵:

$$E(t) = E_0 \sum_{-\infty}^{\infty} J_n(\delta) e^{i(\omega + n\omega_m)t}, \quad (2)$$

we see that the beam contains frequency side bands in increments of ω_n , which extend out to approximately $\pm \delta \omega_m$, at which point the mode amplitudes (J_n) begin to approach zero. Formally, Eq. (2) also contains a factor $\exp(i k_n z)$ where $k_n = (\omega + \omega_n)/c$; the time variable has actually been replaced by $t - z/c$.

2. Bandwidth Dispersion

A crucial element of SSD is that a large number of the DPP elements must be irradiated by different frequencies at each instant of time. The E-O phase-modulated beam, by itself, would not be adequate for SSD, because at any time all DPP elements would be irradiated by only a single dominant frequency given by the time derivative of the phase in Eq. (1). It remains to disperse the different frequencies in the spectrum across the DPP elements. This can be done, in part, by introducing a spatially varying time delay t_D across the beam in, say, the Y direction of the form $t_D = \alpha Y/\omega_m$. Replacing t by $t + t_D$ in Eq. (1), the time-delayed electric field becomes

$$E_D = E_0 e^{i\omega t + i\delta \sin(\omega_m t + \alpha Y)}. \quad (3)$$

The instantaneous frequency, given by the time derivative of the phase in Eq. (3), now varies across the beam. We see it is not necessary to allow the beams to freely propagate to spatially separate the different frequency components as was previously suggested⁴ for SSD; “color” variation has been obtained already with only angular dispersion of the frequencies, resulting in a variable time delay.

Such a time delay can be conveniently introduced by means of a diffraction grating, as illustrated in Fig. 37.21. The grating will, of course, also introduce an angular dispersion to the different frequency components, which can be found from the Bessel-function expansion of Eq. (3):

$$E_D = E_o \sum J_n(\delta) e^{i(\omega + n\omega_m)t + i n \alpha Y} \quad (4)$$

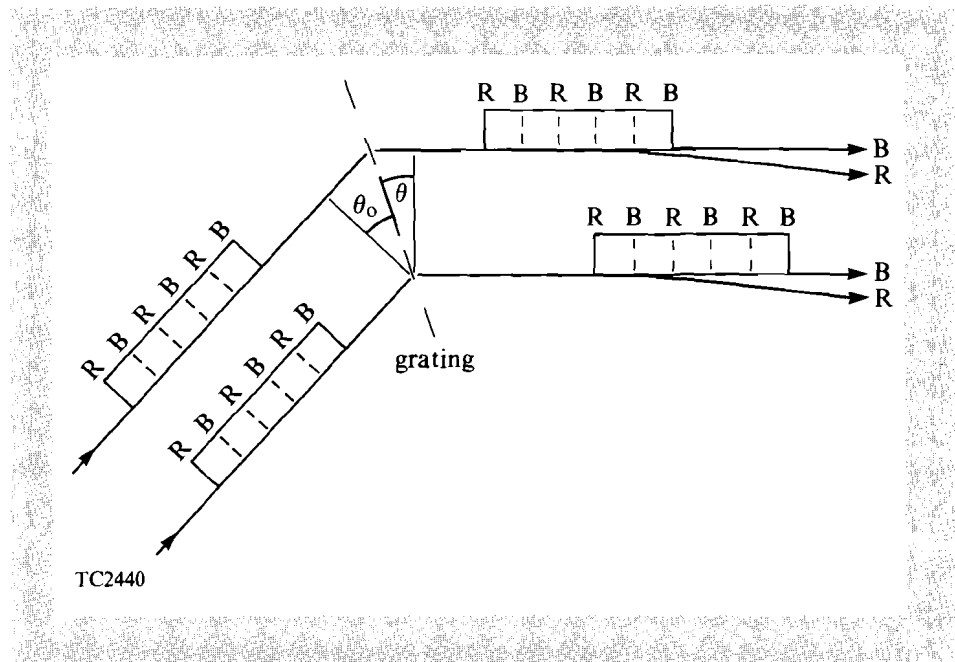
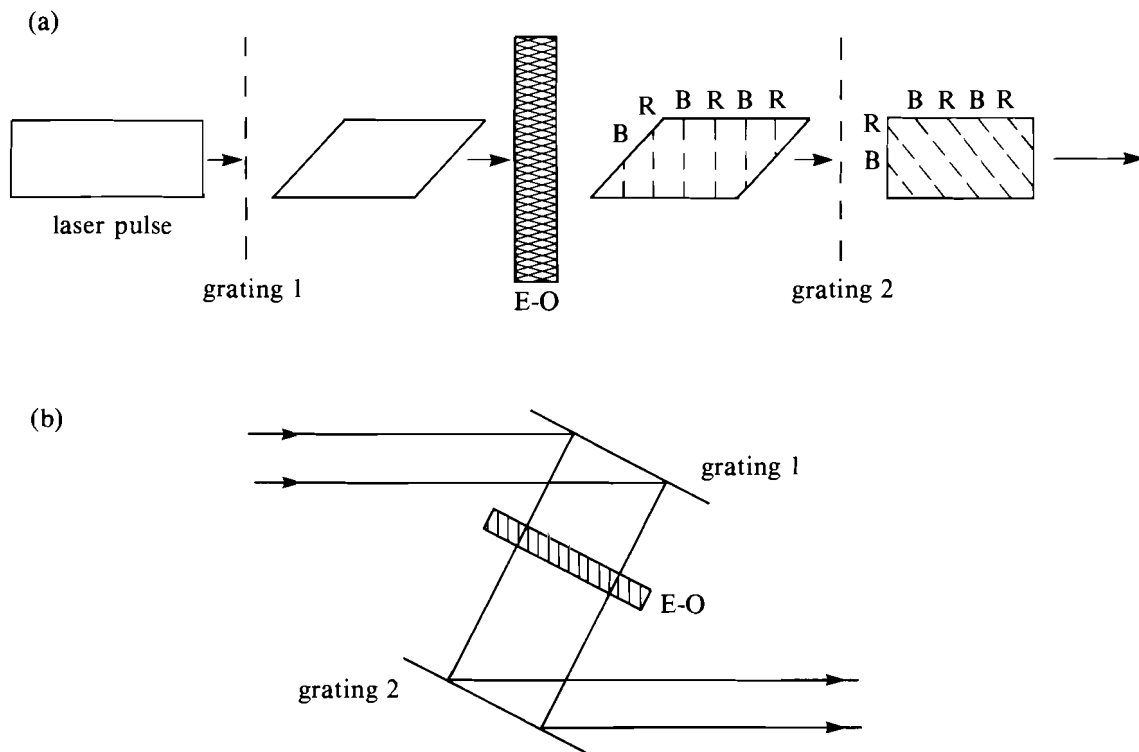


Fig. 37.21
The diffraction grating introduces a time delay across the beam in addition to angular dispersion of the spectrum.

Using the implicit kz dependence in the phase, a contour of constant phase for the n th harmonic is given by $k_n z + \alpha n Y = \text{constant}$. The wave propagates at approximately the angle: $\alpha n/k$ relative to the direction of the fundamental frequency. This angular dispersion is important for high-efficiency frequency conversion as discussed below.

Unfortunately, the time delay, which produced the required frequency variation across the beam, has also distorted the temporal shape of the beam as shown in Fig. 37.21. Not only will the pulse be lengthened, but there will be intensity variations across the beam aperture. This can be corrected by inserting an additional grating before the E-O modulator (Fig. 37.22).



TC2441

Fig. 37.22

The two-grating configuration. (a) Grating 1 introduces a "pre-delay" that compensates for the delay produced by grating 2. By placing the first grating before the modulator, it is possible to correct the time delay without affecting the angular dispersion of the spectrum. (b) A schematic of (a).

When the beam passes through the first grating, its residual bandwidth will, of course, be dispersed; this dispersion is a negligible effect for a typical bandwidth-limited laser beam, and will in any case be corrected by the second grating. The main effect is to introduce a time delay opposite to the one that will be induced by the grating after the E-O modulator. The time-distorted beam passes through the modulator where the bandwidth is imposed. The grating after the E-O modulator now serves a dual purpose: it restores the beam to its correct temporal shape, and it imposes the spatial-frequency variation required for SSD (and also, as discussed below, the correct dispersion for frequency tripling).

3. Diffraction Grating Considerations

The current strategy is to insert the diffraction gratings into the driver, thereby avoiding any additional optical elements at the end of the laser system. The spectral angular divergence imposed in the driver must then be able to propagate through the remainder of the laser and onto the target without significant energy loss or beam distortion. This places an upper bound on the amount of divergence permitted. For instance, if we do not want the spread in the beam at the target plane to be larger than, say, half the target diameter D_T then

$$F\theta \lesssim \frac{1}{2}D_T ,$$

where F is the focal length and θ is the full-angle beam spectral divergence. For OMEGA, $F \approx 60$ cm and, for recent experiments, $D_T \approx 300$ μm . Thus, the largest permitted divergence is ~ 200 μrad , at the 20-cm aperture at the end of the system. Such a divergence can propagate through the OMEGA laser system, if it is introduced near the end of the driver, at the 64-mm stage, where it would have a value three times greater (~ 600 μrad), because the beam divergence changes inversely as the diameter of the beam.

The limit on beam divergence also places an upper bound on the maximum bandwidth that will frequency triple with high efficiency. In order to remain within 10% of the maximum conversion efficiency^{4,6} with the permitted 200- μrad divergence, the bandwidth must not be greater than ~ 2 \AA in the IR. This bandwidth would normally be too small to smooth the laser intensity on the time scale of interest (~ 50 ps) for the OMEGA experiments. But upon frequency conversion, the frequency spread is also tripled. Further, we can take advantage of “color cycling,” as will be discussed below, to further reduce the smoothing time for the long-wavelength interference structure.

We can now determine the grating configuration that would produce the 200- μrad dispersion of the 2- \AA bandwidth. The grating dispersion in the first order is given by⁷

$$\frac{\Delta\theta}{\Delta\lambda} = \frac{1}{\cos(\theta)d} ,$$

where d is the spacing between grooves on the grating and θ is the angle between the transmitted beam and the normal to the grating. A typical value for d is 628 nm. For OMEGA, the beam divergence will be 2.9 times larger at the 64-mm point than it is at the output, i.e., $\Delta\theta/\Delta\lambda = 2.9 \times (200 \mu\text{rad}/2 \text{\AA})$ at the diffraction grating. Therefore, $\cos\theta = 0.54$ and $\theta = 57^\circ$. The minimum length of the grating L can also be determined; it is the beam diameter (58 mm) divided by $\cos\theta$, yielding $L = 10.6$ cm. Gratings with these parameters have been obtained.

4. “Color” Cycling

The time delay across the grating can be used further to our advantage. Fig. 37.22 shows that if the E-O modulation time τ ($=2\pi/\omega_m$) is shorter than the time delay t_D , then all the “colors” will cycle across the beam more than once at each instant in time. (More correctly, one cycle from the “reddish” to “bluish” components of the bandwidth occurs in 0.5τ .) Thus, instead of the “red-blue” variation being distributed from one end of the DPP to the other, it can be distributed over smaller regions of the DPP, so that nearest elements will have a larger frequency difference and their average interference pattern will smooth in a shorter time. For instance, with $1.5 \tau = t_D$, the smoothing time for nearest neighbors is three times shorter than if there had been only one color cycle. The price paid is that more

distant DPP elements will have the same color and their interference pattern will not smooth at all. However, the interference between distant elements produces shorter-wavelength structure that can be smoothed more easily within the target by thermal conduction of the deposited laser energy. The effect of color cycling is qualitatively similar to that produced by repeated echelon steps in the ISI technique.²

To calculate the E-O modulation frequencies that will produce different amounts of color cycling, we first determine the delay time. From Fig. 37.21,

$$t_D = L|\sin\theta + \sin\theta_o|/c, \quad (5)$$

where θ_o is the incident angle of the beam on the grating. The grating dispersion was chosen so that $\theta_o = \theta$ to prevent beam distortion. The incident angle is found from the usual grating equation⁷:

$$|\sin\theta_o + \sin\theta| = \frac{\lambda}{d}. \quad (6)$$

Substituting Eq. (6) into Eq. (5) yields

$$t_D = \frac{L}{c} \frac{\lambda}{d}. \quad (7)$$

For the above values of L and d , and for $\lambda = 1\text{-}\mu\text{m}$ laser light, the delay time t_D is 590 ps. This is approximately the pulse width for current OMEGA experiments, so that the pulse shape after the first grating in Fig. 37.22 will be highly distorted. For the example of three color cycles in the transverse direction across the beam ($\tau = 0.67 t_D$), the modulation frequency $\nu_m (= 1/\tau)$ is 2.5 GHz. The required modulation amplitude δ can also be determined by the following argument. The frequency spread $\Delta\nu$ produced by the 2-Å IR bandwidth is $\Delta\nu = \Delta\lambda c/\lambda^2 = 60$ GHz. The frequency bandwidth produced by E-O modulation is $\Delta\nu = 2\delta\nu_m$ [see discussion of Eq. (2)]. Thus, the modulation amplitude is $\sim 4\pi$ for $\nu_m = 2.5$ GHz.

Simulation Results

To calculate the total electric field on the target (i.e., laser focal plane), we use scalar diffraction theory⁸ to propagate the beam from the phase plates. The beam is first decomposed into its individual frequency components; each frequency is transported separately and then summed in the focal plane. The initial amplitude of each frequency component is determined by the frequency-tripling process.

For a model of the frequency-tripled laser light, we use the following physical argument. The E-O broadened light is oscillating from “red” to “blue” such that at any instant of time only a small frequency range is dominating. The entire small range is approximately phase matched to the crystal because of the angular dispersion of the grating, and high-efficiency conversion should occur.

This process was calculated using the approximations discussed in Ref. 9. Figure 37.23(a) shows the initial 2-Å bandwidth given by Eq. (2), and Fig. 37.23(b) shows the calculated tripled spectrum. The frequency spread has tripled; the shape of the spectrum is given by Eq. (1) with both ω and δ tripled. This result would not apply to the general case of broad-bandwidth light where mode-mode interactions might degrade the conversion efficiency.

Thus, the electric field for the E-O-broadened, frequency-tripled light used here is assumed to be

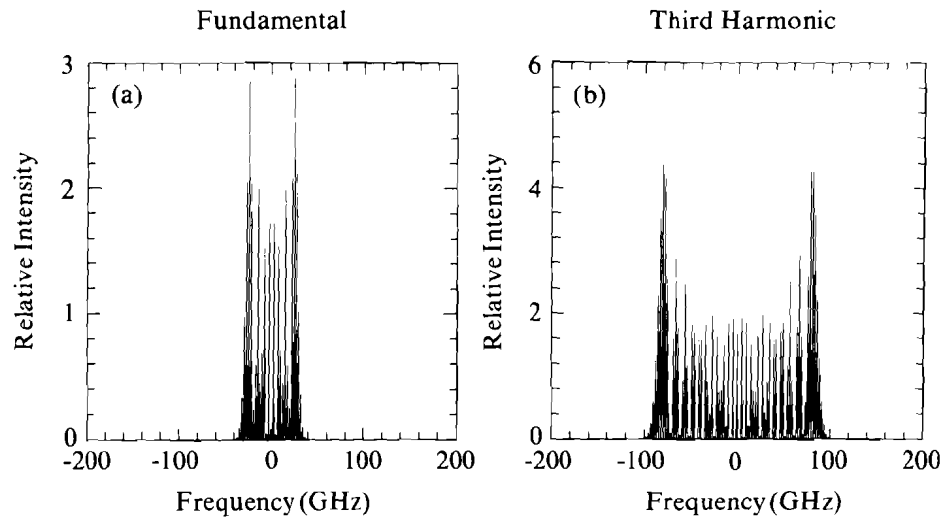
$$E_{3\omega} = e^{i3\omega t + i3\delta \sin(\omega_m t + \alpha Y)}$$

The scalar amplitude of this wave in the focal plane, after passing through the phase plate, is

$$U(x,y) = U_0 e^{i3\omega t}$$

Fig. 37.23
Calculation of the intensity spectrum showing bandwidth tripling upon frequency tripling of a phase-modulated pulse. The slight broadening of each spectral line is due to the finite pulse width of 700 ps used in the calculation.

$$\begin{aligned} & \times \sum_{KL} \sum_n J_n(3\delta) e^{i(n\omega_m t - 2n\gamma L - 2Lq - 2Kp + \phi_{KL})} \\ & \times \frac{\sin(n\gamma + q_n)}{n\gamma + q_n} \frac{\sin p_n}{p_n}, \end{aligned} \tag{8}$$



- E-O phase-modulated beam: $\nu = 2.5 \text{ GHz}$, $\delta \approx 4 \pi$
TC2553

where K, L corresponds to a DPP element, and ϕ_{KL} is the phase imposed by that element. The variables (p_n, q_n) are related to the coordinates (x, y) in the focal plane by

$$(p_n, q_n) = (x, y)k_n \Delta / 2F ,$$

where k_n is the wave number, Δ the distance between phase-plate elements, F the focal length, and $\gamma = \alpha \Delta / 2$.

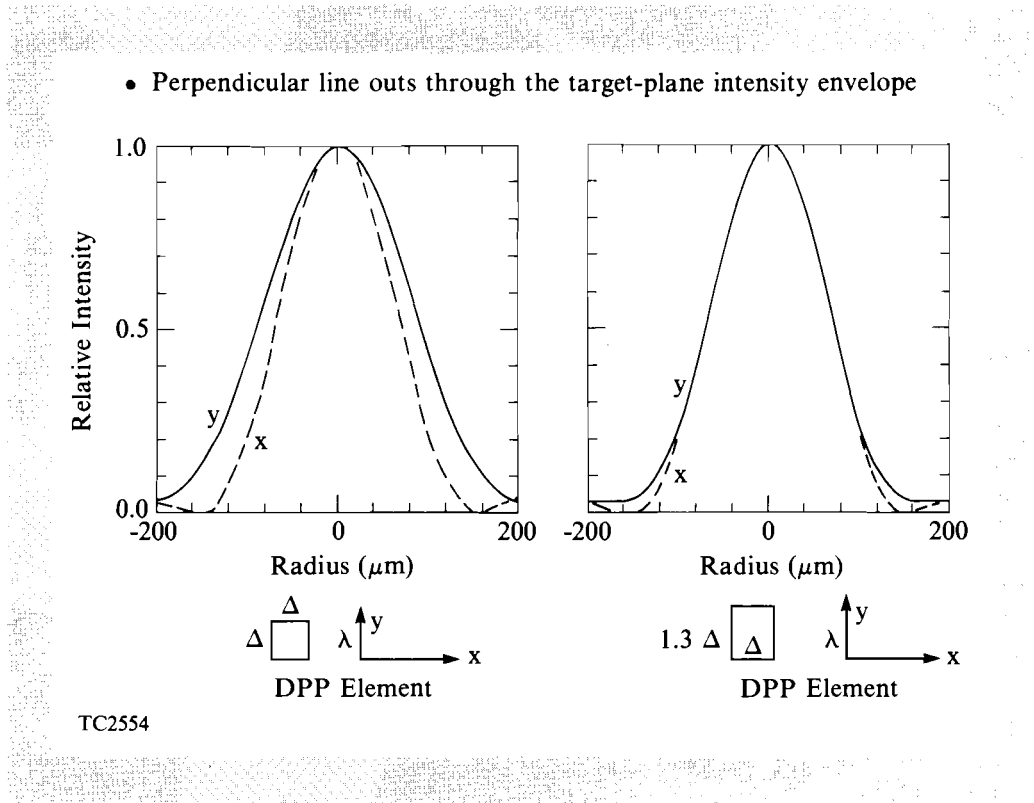
One effect of the spectral angular dispersion is to shift the center of the diffraction envelope for each mode in the q (y) direction. The envelope is no longer the same in the x and y directions; this can introduce long-wavelength modes of irradiation nonuniformity. For the small bandwidth used here, the distortion is relatively small and can be compensated for by using rectangular DPP elements so that the ratio of x to y length is ~ 0.75 (Fig. 37.24). This reduces the diffraction size of the beam in the y direction to approximately compensate for the spread caused by spectral dispersion. The effect on Eq. (8) is to multiply p_n by 0.75.

Fig. 37.24

Correction of the beam ellipticity, in the target plane, by elongating the phase-plate elements in the direction of frequency dispersion. This reduces the diffraction spread in that direction, in part compensating for the spectral dispersion.

The time-averaged, single-beam intensity in the focal plane is

$$I(x, y) = \frac{1}{\Delta t} \int_0^{\Delta t} |U|^2 dt .$$



The intensity on target is the superposition of 24 such intensity patterns. Figure 37.25 shows the rms energy-deposition nonuniformity as a function of the averaging time Δt . The deposited energy was assumed to be smoothed by thermal conduction over 1% of the target radius, which is a conservative estimate; computer simulations of OMEGA experiments show smoothing distances many times larger.

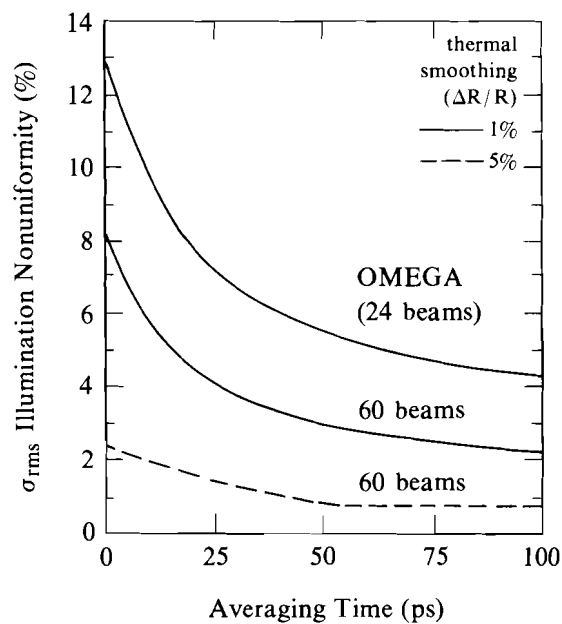
The nonuniformity without SSD ($\Delta t = 0$) is $\sim 12\%$ for the assumed amount of thermal smoothing. SSD, with the 2-Å IR bandwidth and 2.7-GHz modulation frequency, reduces the nonuniformity by factors of 2 to 3 in averaging times of 25–50 ps. The nonuniformity asymptotes to about 4% rms. This residual nonuniformity has two sources. First, bandwidth is dispersed only in the y direction so that all phase-plate elements in the x direction have the same frequency (for a given y); these will form a time-independent interference structure. Second, the oscillating bandwidth causes the interference pattern to repeat after each modulation cycle.

For comparison, results are also shown in Fig. 37.25 for increasing the number of beams and increasing the smoothing distance. A 60-beam configuration can reduce the nonuniformity by a factor of ~ 2 , and increased smoothing ($\Delta R/R = 5\%$) reduces σ_{rms} by another factor of 2.

Although the resultant uniformity is not perfect, the predicted factor of 2 to 3 reduction in σ_{rms} could significantly improve results for OMEGA high-density experiments, and this improvement can be attained with relatively simple modifications of the laser system.

Fig. 37.25

The relatively simple variation of SSD reduces the time-averaged nonuniformity by factors of 2 to 3 in averaging times of 25–50 ps. A 2-Å IR bandwidth was used, and a thermal-smoothing distance of only 1% of the target radius was assumed. Increasing the number of beams from 24 to 60 reduces the nonuniformity by a factor of ~ 2 , and increasing the smoothing distance to 5% of the radius, which is consistent with computer simulation, reduces σ_{rms} by an additional factor of 2.



TC2544

Summary

A relatively simple form of SSD is being investigated for implementation on OMEGA. It is simple in the sense that all new optical elements are installed in the driver, and no additional components are required at the end of the system. An E-O frequency-modulated pulse is used for the bandwidth to prevent the formation of high-intensity spikes that could damage the laser glass, as might occur with a chaotic form of bandwidth. The essential spatial variation of colors on the DPP and angular dispersion for frequency tripling is accomplished with a set of diffraction gratings that take advantage not only of the dispersion properties of the gratings but also their time-delay characteristics.

The same features that make this technique relatively simple also limit the maximum bandwidth to $\sim 2 \text{ \AA}$ for OMEGA. (The bandwidth could be increased to $\sim 4 \text{ \AA}$ without increasing the spectral dispersion, and it will result in only about a 15% reduction in frequency-conversion efficiency.) However, even with 2 \AA , adequate smoothing times can be achieved because this bandwidth is tripled upon frequency conversion and because we can employ color cycling. Computer simulations show that this variation of SSD can reduce the rms nonuniformity on OMEGA by factors of 2 to 3 in averaging times of 25–50 ps.

Even further improvements in uniformity are possible with SSD, but it would involve spatial dispersion of frequencies; in contrast, only angular dispersion was considered here. The spatial dispersion could be more difficult to implement and would require additional lenses around the tripling crystals for optimal conversion efficiency. Hybrids are also possible, with spatial dispersion in one direction and angular dispersion in the other. Such variations of SSD are presently under investigation.

ACKNOWLEDGMENT

This work was supported by the U.S. Department of Energy Office of Inertial Fusion under agreement No. DE-FC03-85DP40200 and by the Laser Fusion Feasibility Project at the Laboratory for Laser Energetics, which has the following sponsors: Empire State Electric Energy Research Corporation, New York State Energy Research and Development Authority, Ontario Hydro, and the University of Rochester. Such support does not imply endorsement of the content by any of the above parties.

REFERENCES

1. LLE Review **33**, 1 (1987).
2. Y. Kato *et al.*, *Phys. Rev. Lett.* **53**, 1057 (1984).
3. R. H. Lehmburg, A. J. Schmitt, and S. E. Bodner, *J. Appl. Phys.* **62**, 2680 (1987).
4. LLE Review **36**, 158 (1988).
5. A. Yariv, *Quantum Electronics*, 2nd ed. (John Wiley & Sons, Inc., New York, 1975), Sec. 14.4.